


# Risk Assessment of Water Inrush in an Underground Coal Mine Based on GIS and Fuzzy Set Theory

Binbin Yang<sup>1</sup> · Wanghua Sui<sup>1</sup>  · Lihong Duan<sup>2</sup>

Received: 29 September 2016 / Accepted: 8 May 2017 / Published online: 20 May 2017  
© Springer-Verlag Berlin Heidelberg 2017

**Abstract** A systematic method was developed to evaluate the risk of water inrush through a coal seam floor using the geographic information system (GIS) and the fuzzy set theory. The main geological and hydrogeological indicators that control water inrush were first considered using a fuzzy mathematics approach, in which fractal analysis was carried out to quantify the fault's characteristics. The degree of membership was determined using GIS, the weight of every factor was considered by calculating the entropy in accordance with Shannon's information entropy theory, and the level of risk of the evaluated object was derived using the maximum membership principle. The approach was validated by a case study at the Chensilou mine in Henan Province, China, where the aquifers that underlie an exploitable coal seam,  $\text{II}_2$ , were made impermeable by grouting. Data from Nov. 2014 to April 2016 shows that the risk of water inrush was reduced in Panel 2517 of the  $\text{II}_2$  coal seam, that there were no serious disturbances in this panel and no

groundwater inrush through the floor. This method can be a powerful tool for systematically assessing the risk of water inrush through the floor, since the influence of several factors can be quantitatively considered in accordance with the geological and mining conditions.

**Keywords** Fractal analysis · Fuzzy synthetic evaluation · Information entropy · Grouting · Degree of membership

## Introduction

High water pressure aquifers, high temperatures, and other geological issues associated with mining deep coal seams have greatly complicated the hydrological and geological conditions and increased the likelihood of water inrush. In fact, there are about 250 million tons of coal in northern China, mainly in the Permo-Carboniferous coalfields, that currently cannot be extracted due to the risk of groundwater inrush, due largely to underlying limestone strata that contain a great deal of water (Gu et al. 2010; Li and Zhou 2006).

In the 1950s, a theory for assessing the risk of water inrush was proposed by a Soviet researcher, V.D. Slesarev (1948), who likened the mine floor to a beam under a uniform load with both ends fixed. In the 1960s, water inrush was documented in the Fengfeng (Hebei province), Jiaozuo (Henan province), Zibo (Shandong province), and Jingxing (Hebei province) coalfields. The data were analyzed by Chinese scholars and engineers, who primarily focused on the water pressure and thickness of the aquifers as the main factors controlling water inrush (Wang 1977). Consequently, a water inrush coefficient method was proposed, which has been widely used in China to predict the likelihood of an inrush because few

**Electronic supplementary material** The online version of this article (doi:10.1007/s10230-017-0457-1) contains supplementary material, which is available to authorized users.

✉ Wanghua Sui  
suiwanghua@cumt.edu.cn

Binbin Yang  
ybb008008@hotmail.com

Lihong Duan  
dlhcumt@163.com

<sup>1</sup> School of Resources and Geosciences, State Key Laboratory for Geomechanics and Deep Underground Engineering, China University of Mining and Technology, 1 University Rd, Xuzhou, Jiangsu 221116, China

<sup>2</sup> Yongcheng Coal and Electricity Holding Group Co. Ltd, Henan Energy and Chemical Industry Group, Middle Guangming Rd, Yongcheng, Henan 476600, China

factors need to be considered and the parameters can be easily obtained (Liu et al. 1995; Meng et al. 2012; Wei et al. 2010). The relationships among water pressure, aquiclude thickness, and water inrush through a coal seam floor were also examined by Mihael Ribičič (1991).

In this century, there has been an increase in related research using different methods to predict the likelihood of water inrush (Wang and Park 2003). Zhang (2005) proposed that four factors are responsible for controlling an inrush: the strata pressure, size of the mine, geological structure, and water pressure of the underlying aquifers. To study the behavior of aquifuges and the likelihood of an inrush, researchers, including Chen et al. (2012), Guo (2008), Jiang (2011), Zhang et al. (2009), and Zhu et al. (2008), have used numerical models based on fluid–solid coupling. The hydro-mechanical coupling theory has been used to determine the effects of water inrush through coal seam floors, and the distribution of stress in the floor has been numerically simulated (Kong et al. 2007; Lu and Wang 2015). The inrush mechanism through a fault has been described (Han et al. 2009; Huang et al. 2012; Wang and Miao 2006; Zhu et al. 2014), and the effect of the amount of water in the aquifers was considered (Shi et al. 2014). Data on the characteristics of the water flow fracture zone or failure of the coal seam floor have been obtained by field monitoring, as well as by physical and numerical simulation experiments. Measurements that predict and prevent water disasters have also been put forward (Sun et al. 2008; Yuan et al. 2015; Wang et al. 2009, 2015). In addition, various formulations have been proposed to assess the risk of water inrush in coal mines over the past few decades, such as the use of the Fisher's discriminant model, grey system theory, fuzzy mathematics theory, attribute mathematics theory, fuzzy Delphi analytic hierarchy process, and grey relational analysis (Chen et al. 2016; Dong et al. 2012; Li et al. 2015; Qiu et al. 2016; Wang et al. 2008, 2012; Wu and Zhou 2008; Wu et al. 2011, 2013). Compared to the coefficient method commonly used in China, these methods focus more on the relationships between different aspects of uncertainty in assessing the probability of water inrush.

Although there have been many methods developed to assess the risk of water inrush in coal mines, no one has considered the spatial characteristics of the factors that affect the occurrence of water inrush and attempted to quantify the relationship between water inrush and influential factors, especially the effects of grouting. This paper therefore provides a new method that combines the use of the geographic information system (GIS) and the fuzzy set theory, in which the main indicators that control water inrush are qualitatively and quantitatively considered and analyzed.

## Methods

Zadeh (1965) first proposed the notion of fuzzy sets, which are sets with elements that have different degrees of membership. The concept was then widely applied and further developed by others (e.g. Kaufmann and Gupta 1988; Li et al. 2014). Groundwater inrush from the mine floor, as the evaluated object, has nonlinear dynamic characteristics. It is affected by many complex factors, which are uncertain, random, and fuzzy. Water inrush cannot be determined by using classical mathematical modeling due to fuzziness (uncertainty). The degree of membership of each factor of an evaluated object is therefore constructed and assessed by using a fuzzy synthetic evaluation method based on fuzzy sets. A quantitative method based on GIS and the fuzzy set theory to assess water inrush was thus developed with the following steps.

1. A set of indicators is established: The set of indicators is a common set composed of all the factors that affect the evaluated object. It is defined as:  $U = \{u_1, u_2, \dots, u_i\}$ , where  $u_i$  ( $i = 1, 2, \dots, n$ ) is the  $i$ th factor in the set of indicators.
2. An evaluation set is established: The evaluation set contains all the possibilities of the evaluation results which are obtained by evaluating the target objects. The evaluation set is defined as:  $V = \{v_1, v_2, \dots, v_j\}$ , where  $v_j$  ( $j = 1, 2, \dots, n$ ) is a possible evaluation result.
3. The weight matrix is determined: In the fuzzy synthetic evaluation system, each factor has a different role with a different weighting coefficient. The weight set is:  $A = (a_1, a_2, a_3, \dots, a_i)$ , where  $a_i \gg 0$  is the weight of the  $i$ th factor and  $\sum a_i = 1$ ,  $a_i$  ( $i = 1, 2, \dots, n$ ).

The weight can be determined by using the entropy concept from information theory, in which entropy is a measurement of uncertainty (Li et al. 2011; Núñez et al. 1996; Wu et al. 2015; Zou et al. 2006). In considering the uncertainty of the fuzzy synthetic evaluation method in calculating multiple factors and neglect of their relationship with water inrush, a weight evaluation process that uses the entropy method is introduced.  $R' = (r'_{ij})_{n \times m}$  is defined as a set of normalized indicator values.

$$r''_{ij} = \frac{r'_{ij}}{\sum_{i=1}^n r'_{ij}}, \quad i = 1, 2, \dots, n; j = 1, 2, \dots, m \quad (1)$$

The information entropy of the  $j$ th factor can be calculated by:

$$E_j = -\frac{1}{\ln n} \sum_{i=1}^n r''_{ij} \ln r''_{ij}, \quad j = 1, 2, \dots, m \quad (2)$$

Specifically, if  $r'_{ij} = 0$ ,  $r'_{ij} \ln r'_{ij} = 0$ . The weight vector  $w = (w_1, w_2, \dots, w_n)$  of the set of indicators can be obtained from:

$$w_j = -\frac{1 - E_j}{\sum_{k=1}^n (1 - E_k)} \quad (3)$$

4. A single factor evaluation and fuzzy relationship matrix based on the GIS are established. The principle behind fuzzy logic is to map each point in the input space to a membership value in the interval  $[0, 1]$  so that the degree of truth can be defined more rationally (Zadeh 1965). Thus, the degree of membership of a single factor can be confirmed based on the GIS to obtain a single factor evaluation set:

$$R_i = (r_{i1}, r_{i2}, \dots, r_{ij})(i = 1, 2, \dots, m)(j = 1, 2, \dots, n) \quad (4)$$

where  $i$  is the number of elements in the set of indicators,  $r_{ij}$  is the degree of membership of an object to  $v_j$ , and  $j$  is the number of elements in the evaluation set.

Mandelbrot (1979) coined the term ‘fractal’ and identified four components that form the basis of the fractal theory: relationships, patterns, emergence, and iterations (Fryer and Ruis 2004). These fractal characteristics are measured using fractal analysis and the changes in the scale of a pattern are indicated by a ratio called a fractal dimension. Here, the complexities of the fault distribution and the maturity of the tectonic evolution are quantitatively explained. The fractal dimension in the spatial distribution of faults is a combined factor of fault dimension and compound modes. There is an important relationship among the fractal structural features of faults, fluid migration, and structural activity (Berry and Lewis 1980; Okubo and Aki 1987; Scholz and Aviles 1985). The most rigorous definition of fractal dimension is the Hausdorff Besicovitch dimension because it is defined over a measure of space, and applied to denote a fractal set (Mandelbrot 1983, 1986a, b). One of the properties of a fractal is its self-similarity; a smaller component of an object when magnified is seen to be similar in shape to its parent object. The Hausdorff Besicovitch dimension of a fractal set that has the same similarity dimensions can be easily determined. Previous research work by Xu et al. (1996) that examined fractal dimensions found that the degree of the complexity of faults are revealed in their similarity dimensions.

The research object here has self-similarity characteristics that could be divided into  $N$  units. The similarity dimension is then defined as:

$$D_s = -\frac{\log N(r)}{\log(r)} \quad (5)$$

where the  $N(r)$  is the number of grids that cross the fault trace, and  $r$  is the similarity ratio of a square grid.

There are many methods available to establish membership functions, such as the fuzzy statistical and Delphi methods. The forms of membership functions include: normal, triangular fuzzy number, lower semi-trapezoid, trapezoidal, and ridge (Chang et al. 2000; Dombi 1990; Klir and Yuan 1995). In this study, the degree of membership was determined using GIS to quantify thematic maps with drawing, mesh generation, and interpolation tools, which provides a data attribute list for the factors. The spatial variation characteristics of each factor can then be obtained.

Some of the indicators in a fuzzy synthetic evaluation model have direct proportional relationships with the evaluated object, and these indicators are then defined as benefit indicators (larger indicator values means reduced risk). Conversely, indicators that do not have direct proportional relationships with the evaluated object are defined as cost indicators; larger indicator values means increased risk (Liu and Qiu 1998). To eliminate the effects of dimensions between the indicators, each factor value  $a_{ij}$  is normalized using the following formulas:

$$\begin{cases} r_{ij} = \frac{a_{ij}}{\max_i \{a_{ij}\}}, & i = 1, 2, \dots, n; j \in \{benefit\} \\ r_{ij} = \frac{\min_i \{a_{ij}\}}{a_{ij}}, & i = 1, 2, \dots, n; j \in \{cost\} \end{cases} \quad (6)$$

where  $r_{ij}$  is non-dimensional data and  $a_{ij}$  is the original data.

There are many data classification methods provided in ArcGIS for statistical mapping, such as equal interval and quartile/even distribution (Coulson 1987; Evans 1977; Simpson and Human 2008). Data values can be classified according to the breaks or gaps that naturally exist in the data, or in accordance with the natural breaks method (Jenks 1963), which is provided in ArcGIS as a means of data classification. The calculation principle for the natural breaks method is defined as:

$$SSD_{i...j} = \sum_{k=i}^j (A[K] - mean_{i...j})^2 \quad (7)$$

where  $SSD_{i...j}$  is the calculation of the variances;  $i, j$  is the sequence number of a classification;  $A[K]$  is the value set of a classification; and  $K = i...j$ ;  $mean_{i...j}$  is the mean value of a classification. With the calculation of different classification areas in the non-dimensional thematic maps, the degree of membership is defined as:

$$r_{ij}(x) = \frac{S_{ij}}{S} \quad (8)$$

where  $r_{ij}(x)$  is the degree of membership of  $v_j$  and  $S_{ij}$  is the area of  $j$ th classification in the  $j$ th indicator thematic maps. By arranging the degree of membership of each factor evaluation set in rows, the single factor evaluation matrix can be expressed as:

$$R = \begin{bmatrix} r_{11} & r_{12} & \cdots & r_{1n} \\ r_{21} & r_{22} & \cdots & r_{2n} \\ \vdots & \vdots & \ddots & \vdots \\ r_{m1} & r_{m2} & \cdots & r_{mn} \end{bmatrix} \quad (9)$$

where  $n$  is the number of elements in the evaluation set, and  $m$  is the number of elements in the set of indicators.

5. Fuzzy synthetic evaluation of multiple factors: The final evaluation set for multiple factors is defined as:  $B = (b_1, b_2, \dots, b_j)(j=1, 2, \dots, n)$ ,  $B = A * R$ , where “\*” denotes the fuzzy operator, and  $b_j$  is the degree of membership of the evaluated object to the  $j$ th possible evaluated result in the evaluation set when considering the effects of multiple factors. The level of the risk of the evaluated target object can be determined in accordance with the maximum membership principle, which is the synthetic degree of the membership of the evaluated object to the possible evaluation results in the evaluation set, which can be expressed as: if  $A_i \in F(U)$  ( $i=1, 2, \dots, n$ ) is defined, and  $u_0 \in U$ , and if exists  $i_0$ , then:

$$A_{i_0}(u_0) = \max\{A_1(u_0), A_2(u_0), \dots, A_n(u_0)\} \quad (10)$$

The  $u_0$  can relatively belong to  $A_{i_0}$ , which is the maximum membership principle.

## Case Study

### The Chensilou Coal Mine

The Chensilou coal mine is located 10 km north of Yongcheng city in the Henan province in China (Supplementary Fig. 1). The mine is 62.4 km<sup>2</sup> in size with a total geological reserve that amounts to 173 million tons of coal and an anticipated service life of 59.4 years. The area is located in the mid-latitude zone in a semi-humid/semi-arid area with a monsoon-type climate. The mining level is generally between 300 and 900 m below sea level. The II<sub>2</sub> coal seam is the primary mineable coal seam in the mine, which is found in the lower Permian series of the Shanxi Formation. The II<sub>2</sub> coal seam is, on average, 2.45 m thick.

The lithology in the area consists of Middle Ordovician (O<sub>2</sub>), Middle and Upper Carboniferous (C<sub>2</sub>, C<sub>3</sub>), Permian

Stratigraphic Unit		Columnar legend	Lithology	Thickness(m)	Remarks
System	Formation	2m Scale			
Permian	Shanxi Formation	II <sub>2</sub>	Coal	Average(2.5)	Aquiclude
			Sandy mudstone		
			Middle-fine sandstone		
			Mudstone	Average(49.87)	
			Medium sandstone		
	Taiyuan Formation		Sandy mudstone		Aquifer
		L <sub>41</sub>	Limestone	Average(1.85)	
			Medium sandstone	Average(5.92)	
		L <sub>10</sub>	Limestone	Average(2.20)	
			Sandy mudstone	Average(6.57)	
		L <sub>9</sub>	Limestone	Average(5.10)	
			Sandy mudstone	Average(6.35)	
		L <sub>8</sub>	Limestone	Average(13.11)	

Fig. 1 Stratigraphic column that underlies the II<sub>2</sub> coal seam

(P), Neogene (E), and Quaternary (Q) deposits (Fig. 1). The strata has been affected by multiple periods of tectonic movement, folding, and faulting. The geological structure

is probably a monocline striking north-northwest with a little dip to the west-southwest. Along the north–south direction, the folds are the primary feature and the faults are secondary. In contrast, in the east–west direction, the faults dominate. A single horizontal seam in the southern and northern wings was mined using a longwall retreat system.

Panel 2517 of the  $\text{II}_2$  coal seam, which is located in District 5 (see Supplementary Fig. 2), is stable enough to be commercially exploited. Structurally, 50 faults have been exposed during excavation and exploration; of these, 4 are reverse faults, while the others are all normal faults. There are 6 faults with displacements that range between 4 and 7 m, 27 with displacements that range between 1 and 4 m, and 17 with displacements less than 1 m.

The three karst aquifers that underlie the exploitable  $\text{II}_2$  coal seam are upper limestone aquifers of the Taiyuan Formation:  $L_{11}$ ,  $L_{10}$ , and  $L_8$ . The average width of the strata between the top of  $L_{11}$ ,  $L_{10}$ , and  $L_8$ , and the bottom of the  $\text{II}_2$  coal seam is 43.6, 58.6, and 75.8 m, respectively.  $L_{11}$  can be recharged by  $L_{10}$  and  $L_8$  through the rock crevices. The water pressure of the upper limestone aquifers of the Taiyuan Formation under the floor of the  $\text{II}_2$  coal seam is more than 5.8 MPa. Given the complex hydrogeological conditions, grouting must be done to render the coal seam floor impermeable, and the aquifer conditions must be reconstructed to prevent and control water disasters in the coal seam floor (State Administration of Coal Mine Safety 2009).

In Panel 2517, 248 holes were drilled for grouting (Fig. 2). The total water yield and grouting volume in  $L_{11}$ ,  $L_{10}$ , and  $L_8$  were determined after drilling. The proportion of the water yield and grouting volume for each aquifer are listed in Supplementary Table 1.  $L_{10}$  and  $L_8$  are the primary aquifers of concern; with a large volume of water and developed karst fissures,  $L_{10}$  and  $L_8$  can recharge  $L_{11}$ .

### Defining a Set of Factors as Indicators for Synthetic Evaluation

Wu and Zhou (2008) established an index system to assess the occurrence of water inrush when mining above

aquifers. The geological structure, hydrogeological conditions (mainly in the aquifers and aquicludes), and mining process were considered the main indicators that influence water inrush due to the development of karst aquifers (Li et al. 2015; Li and Zhou 2006; Qiu et al. 2016; Wang et al. 2012; Wei et al. 2010; Wu et al. 2011, 2013). The karst aquifers that underlie the exploitable  $\text{II}_2$  seam are the upper limestone aquifers of the Taiyuan Formation in the Chensilou mine. Panels 21,201, 21,301, and 21,302 have been mined safely after grouting reinforcement. The characteristics of the geological structure were quantified by fractal analysis using a similarity dimension.

After grouting, the geological structure is affected by the similarity dimensions of the faults (or fracture zones) and the grouting volume of  $L_{11}$ ,  $L_{10}$ , and  $L_8$  in a comprehensive fuzzy evaluation. The effectiveness of the hydrological barrier is affected by the: thickness of the aquiclude situated between the  $L_{11}$  and the  $\text{II}_2$  coal seam, thickness of  $L_{11}$  and  $L_{10}$ , and thickness of the aquiclude situated between  $L_8$  and the  $\text{II}_2$  coal seam. Since  $L_{11}$  and  $L_{10}$  become aquicludes when grouting is applied, the underlying aquifers are affected by the water pressure of the  $L_8$  aquifers and the water yield and grouting volume of  $L_8$ ,  $L_{11}$ , and  $L_{10}$ . The depths of the mining and failure of the coal seam floor were investigated by using in-situ transient electromagnetic measurements (Christiansen et al. 2009) from the panels that were mined with grouting.

In a comprehensive fuzzy evaluation, the four main indicators include ten factors when grouting is carried out or seven factors when no grouting takes place. The likelihood of water inrush was proposed to be based on:

1. the underlying aquifers: the water yield of  $L_{11}$ ,  $L_{10}$ , and  $L_8$  and the water pressure of  $L_8$  (or  $L_{11}$  when no grouting takes place);
2. the hydrogeological barrier: the thickness of the aquicludes situated between  $L_8$  (or  $L_{11}$  when no grouting takes place) and the  $\text{II}_2$  coal seam when grouting is carried out, and the grouting volume of  $L_{11}$ ,  $L_{10}$ , and  $L_8$ ;

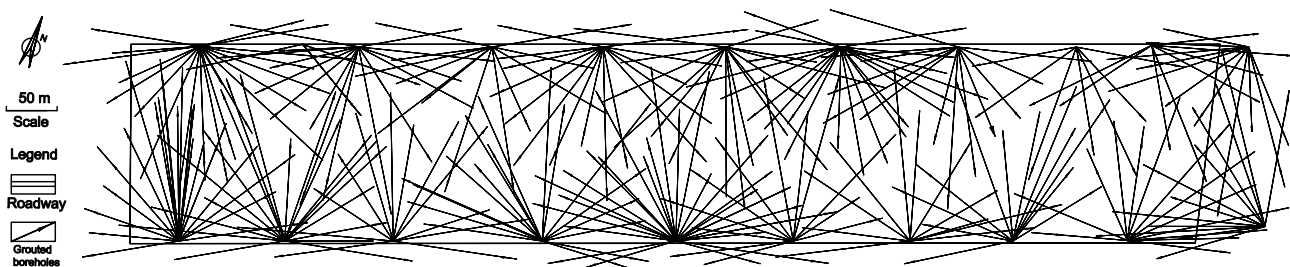


Fig. 2 Layout of grouted boreholes in Panel 2517



- the geological structure: similarity dimensions of the faults (or fracture zones); and
- the mining process: depths of the failure of the coal seam floor.

The factors used as indicators for the synthetic evaluation of water inrush when grouting takes place are:  $U = (U_1, U_2, U_3, U_4, U_5, U_6, U_7, U_8, U_9, U_{10})$  (similarity dimensions of faults or fracture zones, depths of failure of coal seam floor, water pressure of  $L_8$ , thickness of aquicludes situated between  $L_8$  and the  $II_2$  coal seam, water yield of  $L_{11}$ ,  $L_{10}$ , and  $L_8$ , and grouting volume of  $L_{11}$ ,  $L_{10}$ , and  $L_8$ , respectively). The set of factors as indicators for the synthetic evaluation of water inrush when no grouting takes place is defined as:  $U' = (U'_1, U'_2, U'_3, U'_4, U'_5, U'_6, U'_7)$  (similarity dimensions of faults or fracture zones, depths of failure of coal seam floor, water pressure of  $L_{11}$ , thickness of aquiclude between  $L_{11}$  and the  $II_2$  coal seam, and water yield of  $L_{11}$ ,  $L_{10}$ , and  $L_8$ , respectively).

### Establishing Single Factor Evaluation and Fuzzy Relationship Matrix Based on GIS

#### Fractal Analysis Applied to Quantificational Characteristics of a Fault

The study area was divided into 60 squares with 100 m as the length of each side (Fig. 3). Then, the similar ratio is:  $r=1, 1/2, 1/4$ , and  $1/8$ , respectively. The similarity

dimensions were calculated using Eq. (5); the results are listed in Supplementary Table 2. A non-dimensional thematic map of the similarity dimensions was consequently developed using spatial analyst tools and Kriging interpolation and classification (Figs. 4a, 5a).

#### Predicting Depth of Failure: Floor of $II_2$ Coal Seam

In this study, the quantitative relationship between the mining depth and depth of the failure of the coal seam floor was defined using the results of in-situ measurements from the panels that had been mined with grouting (Supplementary Fig. 3) as:

$$h = 6.65 \ln(H) - 28.72 \quad (11)$$

where  $H$  is the mining depth, and  $h$  is the depth of the failure of the coal seam floor.

Prior to reinforcement with grouting, the depths of the failure of the coal seam floor in Panel 2517 were investigated using an empirical formula, in accordance with the regulations of the State Administration of Coal Industry (2000), as follows:

$$h = 0.0085H + 0.1665a + 0.1079L - 4.3579 \quad (12)$$

where  $H$  is the mining depth,  $h$  is the depth of the failure of the coal seam floor,  $a$  is the dip angle, and  $L$  is the panel dip length. The evaluation factors of the depths of the failure of the coal seam floor with and without grouting are quantified and listed in Supplementary Table 3.

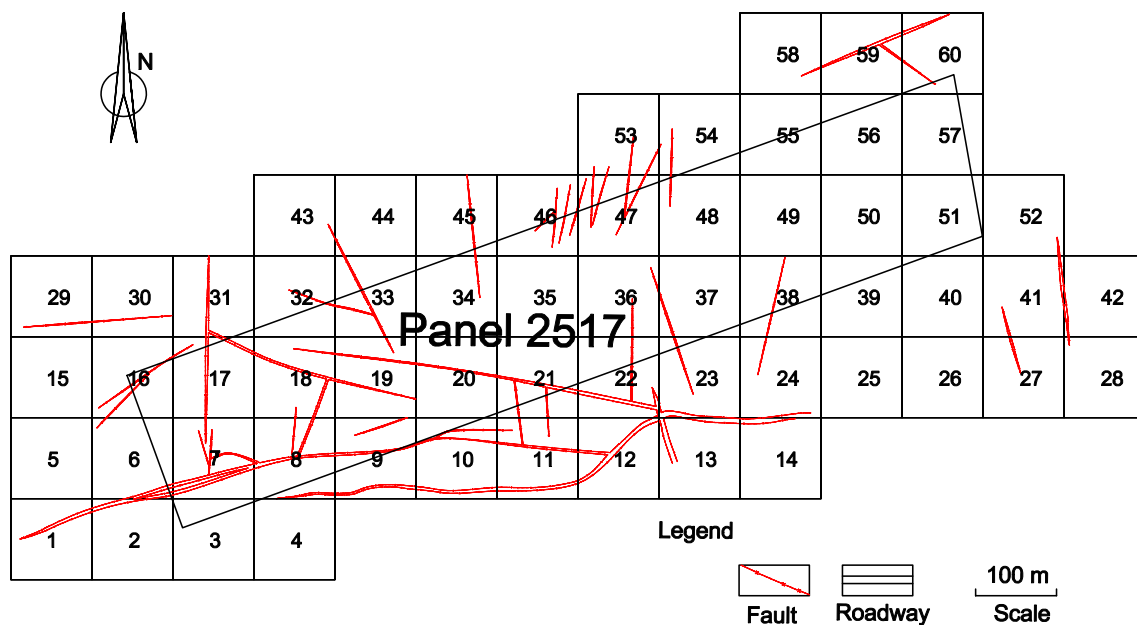
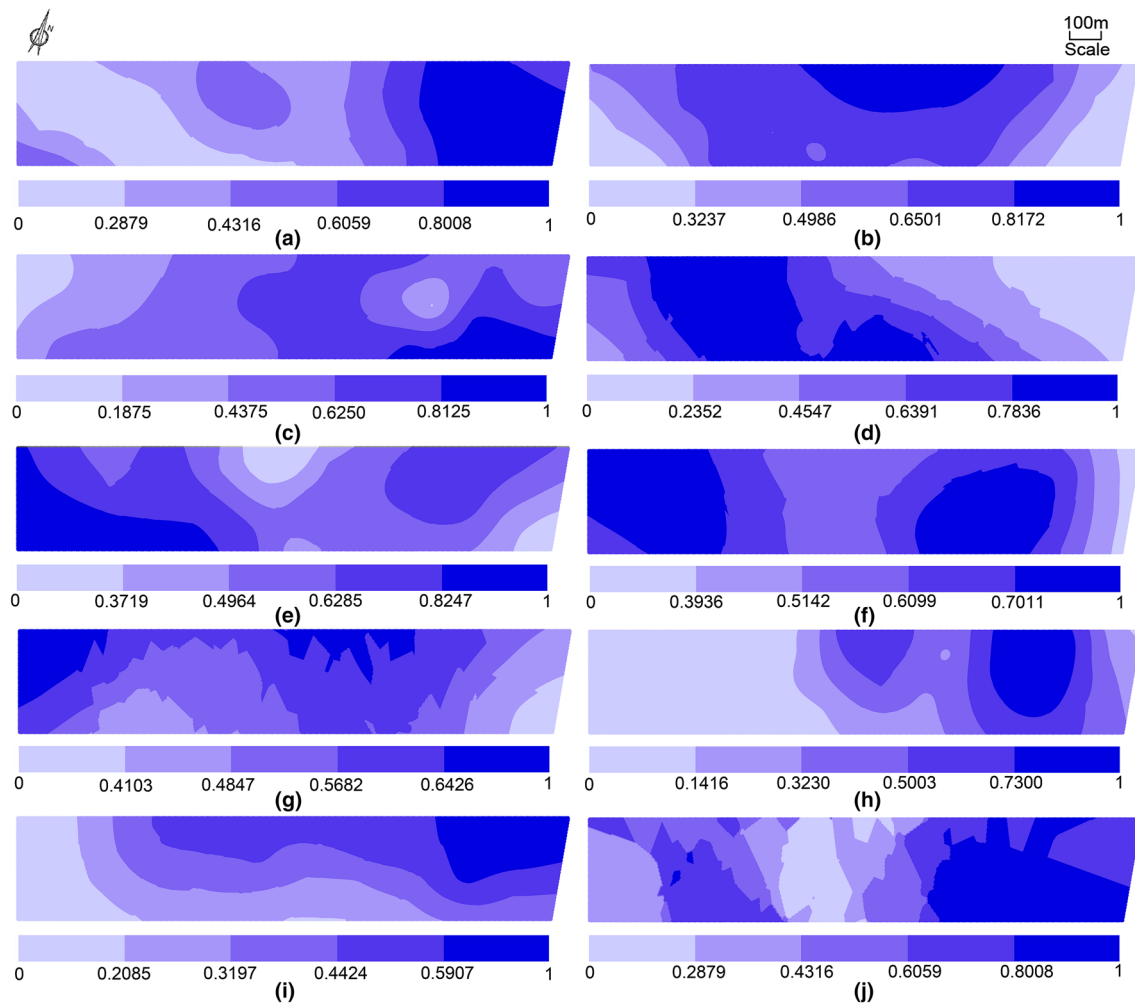


Fig. 3 Faults in Panel 2517



**Fig. 4** Non-dimensional thematic maps of indicators with the use of grouting. **a** Similarity dimensions of faults (or fracture zones); **b** depths of failure of coal seam floor; **c** water pressure of  $L_8$  of Upper Carboniferous Taiyuan Formation under floor of  $II_2$  coal seam; **d**

thickness of aquicludes between  $L_8$  of the Upper Carboniferous Taiyuan Formation and  $II_2$  coal seam; **e** water yield of  $L_{11}$ ; **f** water yield of  $L_{10}$ ; **g** water yield of  $L_8$ ; **h** grouting volume of  $L_{11}$ ; **i** grouting volume of  $L_{10}$ ; and **j** grouting volume of  $L_8$

#### Establishing an Evaluation Set and a Single Factor Evaluation Matrix

Based on previous studies (Li et al. 2013; Wang et al. 2012; Wu and Zhou 2008; Wu et al. 2011, 2013) the risk of water inrush is 5 grades; hence, the evaluation set is:  $V = \{\text{very high, high, medium, low, very low}\}$ . The data for the indicators were collected from 248 holes that were to be grouted. The thematic maps were drawn based on GIS and normalized using Eq. (6). Figures 4 and 5 show the non-dimensional thematic maps that were classified using the natural breaks method (Jenks 1963) with and without grouting, respectively. Each non-dimensional thematic map was divided into five areas:  $\{S_1, S_2, S_3, S_4, S_5\}$ . According to the evaluation set, the degree of membership can be determined by Eq. (8) in

accordance with the non-dimensional thematic maps for the set of indicators. The single factor evaluation matrix is thus determined by arranging the degree of membership of each factor evaluation set with and without grouting, respectively:

$$R = \begin{bmatrix} 0.2362 & 0.2877 & 0.1807 & 0.0890 & 0.2063 \\ 0.1081 & 0.1324 & 0.1424 & 0.4662 & 0.1508 \\ 0.0720 & 0.1427 & 0.4104 & 0.3067 & 0.0681 \\ 0.1824 & 0.1522 & 0.1570 & 0.2093 & 0.2991 \\ 0.0510 & 0.1733 & 0.2582 & 0.3505 & 0.1671 \\ 0.0310 & 0.1475 & 0.2453 & 0.2765 & 0.3997 \\ 0.0276 & 0.2688 & 0.2962 & 0.2812 & 0.1263 \\ 0.4273 & 0.1051 & 0.1765 & 0.1635 & 0.1277 \\ 0.1580 & 0.2119 & 0.2444 & 0.2632 & 0.1225 \\ 0.1139 & 0.1069 & 0.1402 & 0.3996 & 0.2394 \end{bmatrix} \quad (12)$$

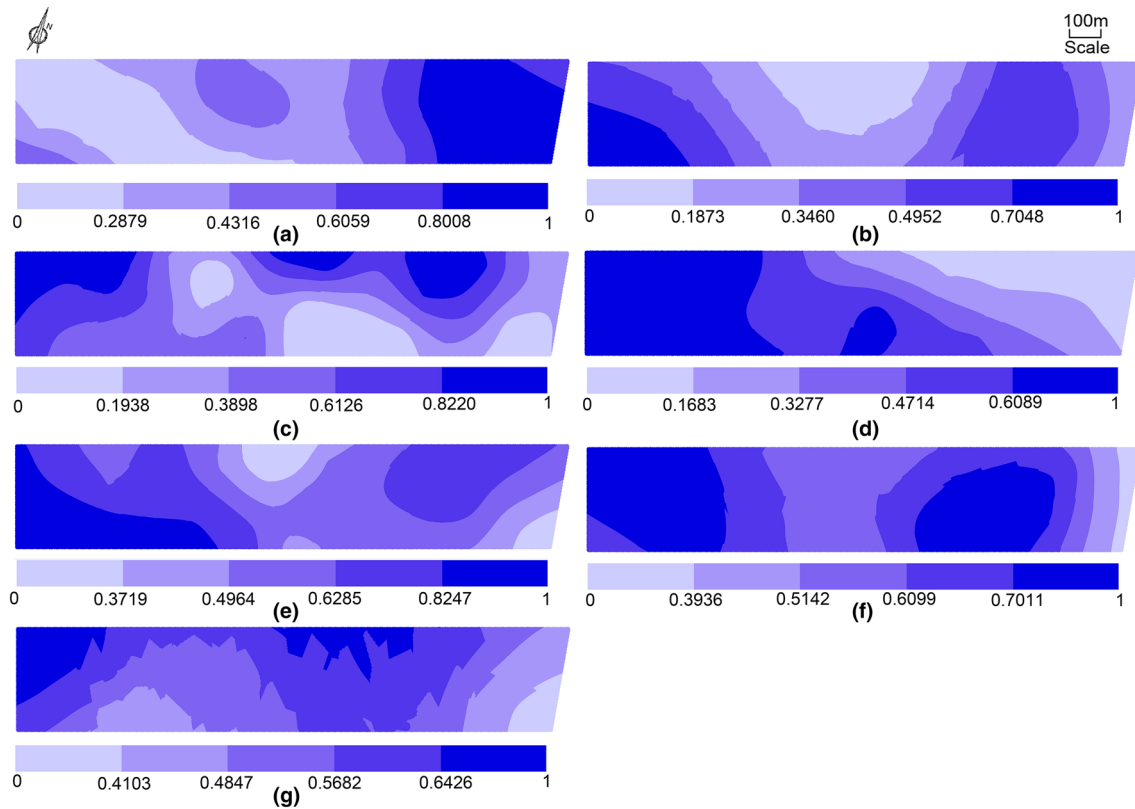


**Fig. 5** Non-dimensional thematic maps of indicators when no grouting takes place. **a** Similarity dimensions of faults (or fracture zones); **b** depths of failure of coal seam floor; **c** water pressure of  $L_{11}$  of Upper Carboniferous Taiyuan Formation under floor of  $II_2$  coal seam;

**d** thickness of aquiclude between  $L_{11}$  of Upper Carboniferous Taiyuan Formation and  $II_2$  coal seam; **e** water yield of  $L_{11}$ ; **f** water yield of  $L_{10}$ ; and **g** water yield of  $L_8$

**Table 1** Weight of each factor with the use of grouting

Factor	Weight
Similarity dimensions of faults (or fracture zones), $U_1$	0.1405
Depths of failure of coal seam floor, $U_2$	0.0528
Water pressure of $L_8$ , $U_3$	0.0942
Thickness of aquicludes, $U_4$	0.0704
Water yield of limestone aquifer	
$L_{11}$ , $U_5$	0.0365
$L_{10}$ , $U_6$	0.0358
$L_8$ , $U_7$	0.0753
Grouting volume of limestone aquifer	
$L_{11}$ , $U_8$	0.2766
$L_{10}$ , $U_9$	0.1179
$L_8$ , $U_{10}$	0.1000

$$R_1 = \begin{bmatrix} 0.2362 & 0.2877 & 0.1807 & 0.0890 & 0.2063 \\ 0.2491 & 0.2688 & 0.2062 & 0.1990 & 0.0769 \\ 0.2932 & 0.1940 & 0.0873 & 0.1463 & 0.1792 \\ 0.2348 & 0.2352 & 0.2664 & 0.1129 & 0.1507 \\ 0.0510 & 0.1733 & 0.2582 & 0.3505 & 0.1671 \\ 0.0310 & 0.1475 & 0.2453 & 0.2765 & 0.3997 \\ 0.0276 & 0.2688 & 0.2962 & 0.2812 & 0.1263 \end{bmatrix} \quad (13)$$

**Table 2** Weight of each factor when no grouting takes place

Factor	Weight
Similarity dimensions of faults (or fracture zones), $U'_1$	0.2294
Depths of failure of coal seam floor, $U'_2$	0.1307
Water pressure of $L_{11}$ , $U'_3$	0.1956
Thickness of aquiclude, $U'_4$	0.2033
Water yield of limestone aquifer	
$L_{11}$ , $U'_5$	0.0596
$L_{10}$ , $U'_6$	0.0584
$L_8$ , $U'_7$	0.1230

### Building the Weight Set

To compute the entropy and weight of each factor in Panel 2517, 38 groups of in-situ measurements and representative calculated data were collected from the southwest, middle, and northeast sides of the panel (see Figs. 4, 5, respectively). The thickness of the aquiclude and the grouting volume of the limestone aquifers were the benefit indicators. The fault or fracture zone, depth of the failure of the coal seam floor, water pressure, and



water yield of the limestone aquifers were the cost indicators. First, the normalized indicator values for grouting/no grouting were obtained from Figs. 4 and 5, and  $R' = (r'_{ij})_{n \times m}$  was constructed to denote the normalized value sets of the indicators. Then each indicator entropy was calculated based on Eqs. (1) and (2). Finally, the weight of each indicator was calculated using Eq. (3) (see Table 1); with grouting, the combined weight set  $A$  is:

$$A = (0.1405, 0.0528, 0.0942, 0.0704, 0.0365, 0.0358, 0.0753, 0.2766, 0.1179, 0.1000)$$

The weight of each indicator is listed in Table 2; without grouting, the combined weight set  $A_1$  is:

$$A_1 = (0.2294, 0.1307, 0.1956, 0.2033, 0.0596, 0.0584, 0.1230)$$

## Results and Discussions

Without grouting, the final evaluation vector was:  $B_1 = A_1 * R_1 = \{0.2001, 0.2148, 0.2117, 0.1819, 0.1719\}$ . There is a high level of risk of water inrush in Panel 2517 if the  $II_2$  coal seam was mined without grouting. With grouting, the final evaluation vector was:  $B = A * R = \{0.2118, 0.1534, 0.2184, 0.2484, 0.1680\}$ .

According to the evaluation results and maximum membership principle, it was concluded that there was a low risk of water inrush in Panel 2517 of the  $II_2$  seam in the Chensilou coal mine, due to the effectiveness of the grouting. The water inrush coefficient is usually calculated by using:

$$T = \frac{P}{M} \quad (14)$$

where  $T$  is the water inrush coefficient;  $P$  is the water pressure of the confined aquifer under the coal seam; and  $M$  is the thickness of the aquiclude. In reality, the effectiveness of the aquiclude after grouting was carried out could not be accurately determined due to its thickness. Hence, the water inrush coefficient cannot be used to predict if water inrush could occur in Panel 2517. To demonstrate the validity of the evaluation results, the transient electromagnetic method was used to examine the resistivity of the coal seam floor in Panel 2517 when grouting was used to reduce permeability. Four different directions were selected to detect water inrush between the upper and lower roadways, respectively (Supplementary Fig. 4). The angles examined between each direction and the coal seam floor are  $-45^\circ$  and  $-60^\circ$  in the upper roadway, and  $-120^\circ$  and  $-150^\circ$  in the lower roadway. Supplementary Fig. 5 shows the isopleth maps of the apparent resistivity of sections in Panel 2517. The electric current distribution in the coal seam floor changes minimally at a depth of 40 m with a good continuity and

there are no places with low resistivity. The electric current distribution at a depth of 40 to 80 m with transverse homogeneity shows that  $L_{10}$  and  $L_{11}$  have turned into aquicludes, and the risk of water inrush in Panel 2517 has obviously been reduced. Since membership functions have different forms, the process of determining and selecting a membership function is subjective. Therefore, GIS was used to determine the degree of membership from non-dimensional thematic maps, as previously discussed, with spatial attributes for the indicators. The use of GIS for determining the degree of membership is more applicable than the use of conventional membership functions. The data from November 2014 to April 2016 indicated that there were no serious disturbances in Panel 2517 that was likely to result in water inrush through the coal seam floor. Thus, the results from the transient electromagnetic method and data taken from the actual mine demonstrate that a fuzzy synthetic evaluation model based on GIS can reliably be used to assess the risk of water inrush.

## Conclusions

The aim of this research was to develop a reliable model to assess the risk of an inrush based on GIS and the fuzzy set theory. A fuzzy synthetic evaluation model was developed and validated in a case study of the Chensilou coal mine in the Henan province of China. The main indicators in the model are the underlying aquifers, hydrologic barrier, geological structure, and mining process.

The possibility of water inrushes in Panel 2517 was affected by ten specific factors when grouting was applied, the: fault or fracture zone, depth of failure of the coal seam floor, thickness of the aquicludes between  $L_8$  of the Upper Carboniferous Taiyuan Formation and the  $II_2$  coal seam, water pressure in  $L_8$  of the Upper Carboniferous Taiyuan Formation under the floor of the  $II_2$  coal seam, water yield of  $L_8$ ,  $L_{10}$ , and  $L_{11}$ , and grouting volume of  $L_8$ ,  $L_{10}$ , and  $L_{11}$ . The quantities of non-dimensional data were processed to eliminate the effects of the different dimensions of the original data. Then, non-dimensional thematic maps for the indicators were constructed by using the natural breaks method provided in ArcGIS. The degree of membership of a single factor was confirmed based on the calculation of different classification areas in the non-dimensional thematic maps. A new weight evaluation process that uses the entropy method based on information theory is proposed.

In a comparison of the level of risk of water inrush before and after grouting by using the water inrush coefficient method, it was found that this approach adequately contributed to predicting or evaluating water inrush by

improving the decision-making process during underground coal mining.

**Acknowledgements** The authors acknowledge the financial support from the National Natural Science Foundation of China under Grant 41472268, the 973 Program under Grant 2013CB227903, a Project Funded by the Priority Academic Program Development of Jiangsu Higher Education Institutions, and the 111 Project under Grant B14021.

## References

- Berry MV, Lewis ZV (1980) On the Weierstrass-Mandelbrot fractal function. *P R Soc Lond A-Cont* 370(1743): 459–484
- Chang PT, Huang LC, Lin HJ (2000) The fuzzy Delphi method via fuzzy statistics and membership function fitting and an application to the human resources. *Fuzzy Set Syst* 112(3): 511–520
- Chen L, Feng X, Xie W, Xu D (2016) Prediction of water-inrush risk areas in process of mining under the unconsolidated and confined aquifer: a case study from the Qidong coal mine in China. *Environ Earth Sci* 75(8):1–17
- Chen LW, Qin Y, Gui HR, Zhang SL (2012) Analysis on probability of water inrush and quicksand in different mining sequences under an unconsolidated alluvium aquifer by fluid-solid coupling theory. *J Coal Sci Eng* 18(1):60–66
- Chen JM, Yang RS (2011) Analysis of mine water inrush accident based on FTA. *Proc Environ Sci* 11:1550–1554
- Christiansen AV, Auken E, Sørensen K (2009) The transient electromagnetic method. *Groundwater geophysics*, Springer, Berlin, pp 179–226
- Coulson MR (1987) In the matter of class intervals for choropleth maps: with particular reference to the work of George F Jenks. *Cartographica* 24(2):16–39
- Dombi J (1990) Membership function as an evaluation. *Fuzzy Set Syst* 35(1):1–21
- Dong DL, Sun WJ, Xi S (2012) Water-inrush assessment using a GIS-based Bayesian network for the 12–2 coal seam of the Kailuan Donghuanuo coal mine in China. *Mine Water Environ* 31(2):138–146
- Evans IS (1977) The selection of class intervals. *T I Brit Geogr* 2(1):98–124
- Fryer P, Ruis J (2004) What are Fractal Systems? <http://www.fractal.org/Fractal-systems.htm>. Accessed 18 June 2004
- Gu XG, Wang JC, Liu YD (2010) Water resistant features of high-risk outburst coal seams and standard discriminant model of mining under water-pressure. *Min Sci Technol* 20(6):797–802
- Guo BH (2008) Numerical analysis on water-inrush process due to floor heave. *J Coal Sci Eng* 14:225–229
- Han J, Shi LQ, Yu XG, Wei JC, Li SC (2009) Mechanism of mine water-inrush through a fault from the floor. *Min Sci Technol* 19(3):276–281
- Hang Y, Zhang GL, Yang GY (2009) Numerical simulation of dewatering thick unconsolidated aquifers for safety of underground coal mining. *Mining Sci Technol* 19(3):312–316
- Huang HF, Mao XB, Yao BH, Pu H (2012) Numerical simulation on fault water-inrush based on fluid-solid coupling theory. *J Coal Sci Eng* 18(3):291–296
- Jenks GF (1963) Generalization in statistical mapping. *Ann Assoc Am Geogr* 53(1):15–26
- Jiang ZH (2011) Numerical analysis of the destruction of water-resisting strata in a coal seam floor in mining above aquifers. *Min Sci Technol* 21(4):537–541
- Kaufmann A, Gupta MM (1988) *Fuzzy Mathematical Models in Engineering and Management Science*. Elsevier Science, North Holland
- Klir G, Yuan B (1995) *Fuzzy sets and fuzzy logic*, vol 4. Prentice Hall, NJ
- Kong HL, Miao XX, Wang LZ, Zhang Y, Chen ZQ (2007) Analysis of the harmfulness of water-inrush from coal seam floor based on seepage instability theory. *J China Univ Mining Technol* 17(4):453–458
- Li PY, Qian H, Wu JH (2011). Application of set pair analysis method based on entropy weight in groundwater quality assessment—a case study in Dongsheng City, northwest China. *E-J Chem* 8(2):851–858
- Li PY, Wu JH, Qian H, Lyu XH, Liu HW (2014). Origin and assessment of groundwater pollution and associated health risk: a case study in an industrial park, northwest China. *Environ Geochem Health* 36(4):693–712
- Li GY, Zhou WF (2006) Impact of karst water on coal mining in North China. *Environ Geol* 49(3):449–457
- Li SC, Zhou ZQ, Li LP, Xu ZH, Zhang QQ, Shi SS (2013) Risk assessment of water inrush in karst tunnels based on attribute synthetic evaluation system. *Tunn Undergr Sp Tech* 38:50–58
- Li LP, Zhou ZQ, Li SC, Xue YG, Xu ZH, Shi SS (2015) An attribute synthetic evaluation system for risk assessment of floor water inrush in coal mines. *Mine Water Environ* 34(3):288–294
- Liu Q (2009) A discussion on water inrush coefficient. *Coal Geol Explor* 37(4):34–38. doi:10.3969/j.issn.1001-1986.2009.04.009 (In Chinese)
- Liu TQ, Chen ST, Chen XH (1995) Preliminary study on steeply inclined coal seam mining under water body. *J Chin Coal Soc* 2(3):1–14 (Chinese)
- Liu SL, Qiu WH (1998) Studies on the Basic Theories for MADM. *Syst Eng Theory Pract* 18(1):38–43. doi:10.3321/j.issn:1000-6788.1998.01.007 (In Chinese)
- Lu YL, Wang LG (2015) Numerical simulation of mining-induced fracture evolution and water flow in coal seam floor above a confined aquifer. *Comput Geotech* 67:157–171
- Mandelbrot BB (1983) *The Fractal Geometry of Nature*. Revised and enlarged edit. W. H. Freeman, New York City
- Mandelbrot BB (1986a) Self-affine fractal sets, I: the basic fractal dimensions. *Fractals in Physics, Proc 6th Trieste International Symp* 1:3–15. DOI:10.1016/B978-0-444-86995-1.50004-4
- Mandelbrot BB (1986b) Self-affine fractal sets, II: length and surface dimensions. *Fractals in Physics, Proc 6th Trieste International Symp* 1:17–20. doi:10.1016/B978-0-444-86995-1.50005-6
- Mandelbrot BB (1979) *Fractals: Form, Chance and Dimension*. WH Freeman, San Francisco
- Meng ZP, Li GP, Xie XT (2012) A geological assessment method of floor water inrush risk and its application. *Eng Geol* 143–144:51–60
- Nguyen QP, Konietzky H, Nguyen QL, Pham NA (2014) Numerical simulation of the influence of water inrush on underground coal mining stability in Vietnam. *Mine Planning and Equipment Selection*, Springer International, Heidelberg, pp 629–636
- Núñez JA, Cincotta PM, Wachlin FC (1996) Information entropy: an indicator of chaos. *Chaos in gravitational N-body systems* (La Plata, 1995). *Celest Mech Dyn Astr* 64(1–2):43–53
- Okubo PG, Aki K (1987) Fractal geometry in the San Andreas Fault system. *J Geophys Res* 92(B1):345–355
- Pang YH, Wang GF, Ding ZW (2014) Mechanical model of water inrush from coal seam floor based on triaxial seepage experiments. *Int J Coal Sci Technol* 1(4):428–433
- Peng SP, Wang JA (2001) *Coal mining safety on confined water body*. China Coal Industry Publ House, Beijing (In Chinese)
- Qiu M, Shi LQ, Teng C, Zhou Y (2016) Assessment of water inrush risk using the fuzzy Delphi analytic hierarchy process and grey

- relational analysis in the Liangzhuang coal mine, China. *Mine Water Environ* 39:1–12
- Ribičič MS, Kočevar M, Hoblaj R (1991) Hydrofracturing of rock as a method of evaluation of water, mud and gas inrush hazards in underground coal mining. *Proc. 4th International Mine Water Assoc Congr* 1:1–12
- Scholz CH, Aviles CA (1985) Fractal dimension of the 1906 San Andreas Fault and 1915 Pleasant Valley faults. *Earthquake. Notes* 55(1):20
- Shi L, Qiu M, Wei W, Xu D, Han J (2014) Water inrush evaluation of coal seam floor by integrating the water inrush coefficient and the information of water abundance. *Int J Mining Sci Technol* 24(5):677–681
- Simpson DM, Human RJ (2008) Large-scale vulnerability assessments for natural hazards. *Nat Hazards* 47(2):143–155
- Slesarev VD (1948) Design of the Optimal Mine Pillars. *Mechanika, Gornoe Delo, Ugletekhizdat, Moscow*, pp 238–261 [In Russian]
- State Administration of Coal Mine Safety (2009) Regulations of preventing water hazards for coalmines. Coal Industry Press, Beijing (**Chinese**)
- State Administration of Coal Industry (2000) Regulations of the coal pillar design for main roadway and coal mining under buildings, water bodies and railways. Coal Industry Press, Beijing (**Chinese**)
- Sun YJ, Xu ZM, Dong QH, Liu SD, Gao RB, Jiang YH (2008) Forecasting water disaster for a coal mine under the Xiaolangdi reservoir. *J China Univ Mining Technol* 18(4):516–520
- Wang MY (1977) Mechanism and prediction of water inrush from coal seam floor in the Carboniferous Permian coal field in Hebei, Shandong and Henan. *Coal Geol Explor* 5:21–32 (**In Chinese**)
- Wang LG, Miao XX (2006) Numerical simulation of coal floor fault activation influenced by mining. *J China Univ Mining Technol* 16(4):385–388
- Wang LG, Miao XX, Dong X, Wu Y (2008) Application of quantification theory in risk assessment of mine flooding. *J China Univ Mining Technol* 18(1):38–41
- Wang JA, Park HD (2003) Coal mining above a confined aquifer. *Int J Rock Mech Min* 40(4):537–551
- Wang JA, Tang J, Jiao SH (2015) Seepage prevention of mining-disturbed riverbed. *Int J Rock Mech Min* 75:1–14
- Wang LG, Wu Y, Sun J (2009) Three-dimensional numerical simulation on deformation and failure of deep stope floor. *P Earth Planetary Sci* 1(1):577–584. doi:10.1016/j.proeps.2009.09.092
- Wang Y, Yang WF, Li M, Liu X (2012) Risk assessment of floor water inrush in coal mines based on secondary fuzzy comprehensive evaluation. *Int J Rock Mech Min* 52:50–55
- Wei J, Li Z, Shi L, Guan Y, Yin H (2010) Comprehensive evaluation of water-inrush risk from coal floors. *Min Sci Technol* 20(1):121–125
- Wu Q, Fan SK, Zhou WF, Liu SQ (2013) Application of the analytic hierarchy process to assessment of water inrush: a case study for the No. 17 Coal Seam in the Sanhejian Coal Mine, China. *Mine Water Environ* 32(3):229–238
- Wu JH, Li PY, Qian H, Chen J (2015) On the sensitivity of entropy weight to sample statistics in assessing water quality: statistical analysis based on large stochastic samples. *Environ. Earth Sci* 74(3):2185–2195
- Wu Q, Liu YZ, Liu DH, Zhou WF (2011) Prediction of floor water inrush: The application of GIS-based AHP vulnerable index method to Donghuantuo coal mine, China. *Rock Mech Rock Eng* 44(5):591–600
- Wu Q, Zhou WF (2008) Prediction of groundwater inrush into coal mines from aquifers underlying the coal seams in China: vulnerability index method and its construction. *Environ Geol* 56(2):245–254
- Wu Q, Xu H, Pang W (2008) GIS and ANN coupling model: an innovative approach to evaluate vulnerability of karst water inrush in coalmines of north China. *Environ Geol* 54(5):937–943
- Xu JP, Sui WH, Gui H, Zhang, YD (2009) Utilizing angular displacement to monitor failure of coal seam floor. *P Earth Planet Sci* 1(1):943–948
- Xu ZM, Sun YJ, Dong QH, Zhang GW, Li S (2010) Predicting the height of water-flow fractured zone during coal mining under the Xiaolangdi Reservoir. *Min Sci Technol (China)* 20(3):434–438
- Xu ZB, Wang JY, Zhang DS, Xie HP (1996) Fractal dimension description of complexity of fault network in coal mines. *J China Coal Soci* 21(4):358–363 (**Chinese**)
- Yao BH, Bai HB, Zhang BY (2012) Numerical simulation on the risk of roof water inrush in Wuyang Coal Mine. *Int J Mining Sci Technol* 22(2):273–277
- Yuan R, Li Y, Jiao Z (2015) Movement of overburden stratum and damage evolution of floor stratum during coal mining above aquifers. *Proc Eng* 102:1857–1866
- Zadeh LA (1965) Fuzzy sets. *Inform Control* 8(3):338–353
- Zhang JC (2005) Investigations of water inrushes from aquifers under coal seams. *Int J Rock Mech Min* 42(3):350–360
- Zhang HQ, He YN, Tang CA, Ahmad B, Han LJ (2009) Application of an improved flow-stress-damage model to the criticality assessment of water inrush in a mine: a case study. *R Rock Mech Rock Eng* 42(6): 911–930
- Zhu QH, Feng MM, Mao XB (2008) Numerical analysis of water inrush from working-face floor during mining. *J China U Min Tech* 18(2):159–163
- Zhu B, Wu Q, Yang J, Cui T (2014) Study of pore pressure change during mining and its application on water inrush prevention: a numerical simulation case in Zhaogezhuang coalmine, China. *Environ. Earth Sci* 71(5):2115–2132
- Zou ZH, Yi Y, Sun JN (2006) Entropy method for determination of weight of evaluating indicators in fuzzy synthetic evaluation for water quality assessment. *J Environ Sci* 18(5):1020–1023